

Detecting vortices in fluid dynamics simulations using computer vision

Thomas Rometsch^{}

Universität Tübingen
Auf der Morgenstelle 10, 72076 Tübingen, Germany
email: thomas.rometsch@uni-tuebingen.de

Abstract. Vortices are patches of fluid revolving around a central axis. They are ubiquitous in fluid dynamics. To the human eye, detecting vortices is a trivial task thanks to our inherent ability to identify patterns. To solve this task automatically, we developed the Vortector pipeline which was used to identify and characterize vortices in around one million snapshots of planet-disk interaction simulations in the context of planet formation. From the emergence of two regimes of vortex lifetime, one of which shows very long-lived vortices, we conclude that future resolved disk observations will predominantly detect vortices in the outer parts of protoplanetary disks.

Keywords. protoplanetary disks – planet–disk interaction – fluid dynamics – methods: numerical

1. Introduction

Protoplanetary disks (PPDs) are flat rotating, mostly gaseous objects that form together with their host stars and are the birthplaces of planets.

Goodman et al. (1987) showed that vortices exist in PPDs by providing an analytical vortex solution of the fluid dynamics equations. Later, vortices were also observed in numerical fluid dynamics models, including models in which the vortex was caused by an embedded giant planet (Godon & Livio 1999; De Val-Borro et al. 2007). Since the advent of high-resolution radio astronomy observations (e.g., with ALMA), non-axisymmetric structures have been observed in protoplanetary disks and interpreted as vortices (van der Marel et al. 2013; Bae et al. 2016; Pérez et al. 2018).

Early numerical modeling relied on the assumption that the temperature in the disk is not changing with time. This assumption of an isothermal disk has the advantage of reducing simulation runtime and reducing physical complexity. In recent years, however, it has become evident that the isothermal assumption results in incorrect features in the disks under certain conditions (Ziampras et al. 2020; Miranda & Rafikov 2020), which is especially relevant for the comparison to resolved disk observations and the interpretation of observed substructures.

To improve the models, the radiative effects in the disk can be modeled using the β -cooling prescription (Gammie 2001). In Rometsch et al. (2021) we used this prescription to model vortices in protoplanetary disks that emerge as a consequence of gap opening by an embedded giant planet.

One challenge in numerical studies of vortices is that vortices are not represented as simulation objects but emerge as a pattern in the velocity field. For a small number of simulations and output snapshots, the detection and characterization might be performed

manually. In our study, we needed to detect vortices in more than 1 000 000 simulation snapshots, which had to be done using a computer algorithm.

In this document, we highlight the approach we took to identify and characterize vortices in our recent study. We also present a prediction about the expected location of vortices as they will be observed with upcoming high-resolution disk observations.

2. Overview

Vortex models.

The motion of a vortex can fundamentally be described by the curl of the velocity of the flow, \vec{v} , which is called vorticity

$$\vec{\omega} = \nabla \times \vec{v}. \tag{2.1}$$

In the case of vortices in protoplanetary disks, the disk motion is approximately Keplerian, meaning the velocity at each radius r away from the star is given by the Keplerian velocity $v \approx v_K = r\Omega_K$, with the Keplerian angular velocity Ω_K . This results in a background vorticity of the disk $\omega_K = \Omega_K/2$. Vortices being formed at the outer edge of a gap carved by an embedded giant planet usually rotate anticyclonically compared to the background disk. Inside an anticyclonic vortex, the vorticity of the fluid is lowered — being anticyclonic motion, it must have the opposite sign compared to the background disk. Associated with an anticyclonic vortex is an increase in mass density.

Considering a vertically integrated disk model (2D) in the $r - \Phi$ plane of cylindrical coordinates centered on the star, vortices have an elliptical shape (a crescent shape in a top-down view on the disk) and the surface density Σ is approximately a Gaussian bell curve in the vortex region, with a different extent in each direction (for an illustrative explanation see Sect 3.1 in [Lin & Pierens \(2018\)](#)),

$$\Sigma(r, \Phi) = \Sigma_p \exp \left(-\frac{(r - r_0)^2}{2\sigma_r^2} - \frac{(\Phi - \Phi_0)^2}{2\sigma_\Phi^2} \right). \tag{2.2}$$

Here, Σ_p is the peak density inside the vortex, r_0 and Φ_0 are the center coordinates of the vortex, and σ_r and σ_Φ are a measure for the extent of the vortex in each direction.

Vortex detection algorithm.

These three characteristics of anticyclonic vortices in disks,

- the local minimum of vorticity,
- the elliptical shape,
- and the Gaussian density peak

are used as the basis for our detection algorithm.

For the detection of vortices in the velocity field, we first compute ω and then divide by Σ to get the vortensity $\varpi = \omega_z / \Sigma$. The additional division by Σ (which peaks inside of the vortex) enhances the contrast between the background disk and the vortex interior, where ω_z has a minimum. To be able to use the algorithm in different scenarios, the vortensity is also normalized to the background vorticity ϖ_K , usually resulting in vortensity values between -1 and 1. This normalization has the benefit of removing the radial variation due to the background profile of Σ and Ω_K .

The first step of the algorithm is the identification of vortex candidates. We use the fact that the vortensity has a minimum inside of the vortex. Thus, iso-value lines of vortensity must be closed around the vortex center. Hence, closed iso-value lines are candidates for a vortex. The iso-vortensity lines are extracted using the computer vision library **OpenCV**.

The second step is to identify possible vortices by their elliptical shape. To compare the contours to ellipses, a fit of the ellipse equation to the contour lines is performed, and the difference between the area of the fitted ellipse and the area enclosed by the closed contour is computed. If the relative difference between the two areas is smaller than a

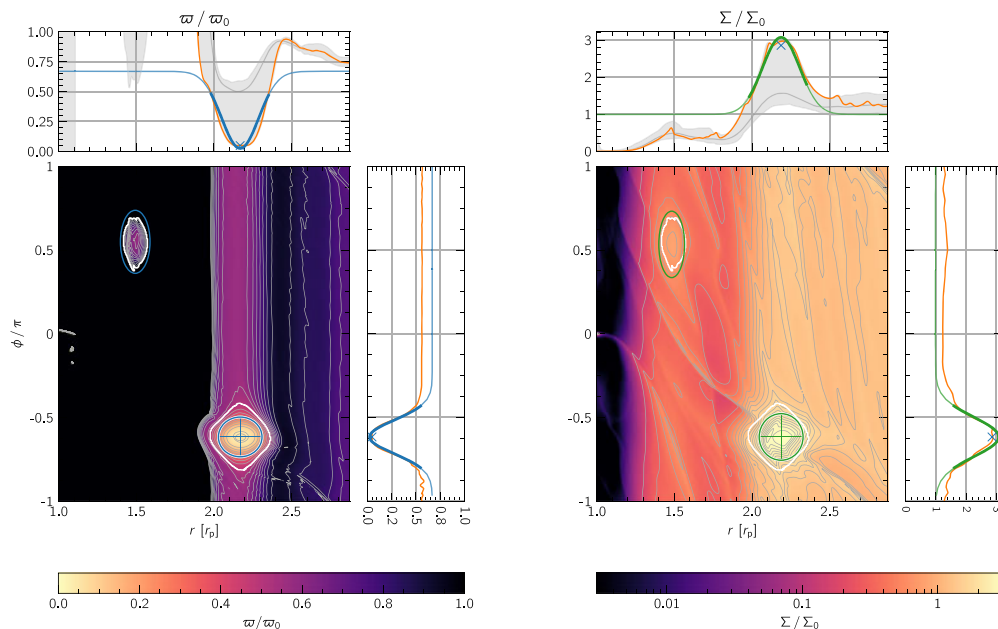


Figure 1. Vortex detection in a planet-disk simulation based on iso-vortensity lines using the *Vortector* utility. Normalized vortensity ϖ/ϖ_K and surface density Σ are shown in the left and right panels, respectively, with iso-value lines in grey. The detected vortices are indicated by the white contour line and the ellipses (corresponding to the FWHM extent). The side panels show cuts through the center of the vortex marked by the crosshair and Gaussian bell curves fitted to the 2D data. Adapted from Fig. B.2 in Rometsch et al. (2021).

threshold (we used 0.122), we consider the contour as a candidate for a vortex. Because multiple iso-value lines might surround a minimum, we only keep the outermost contours that enclose all other contours around the same center.

The final step is to fit the model density peak from Eq. (2.2) to the data inside the candidate contour. An example of the resulting vortex identification for a model from Rometsch et al. (2021) is shown in Fig. 1. Having a fit to the data allows for defining the vortex independent of detection parameters. We defined the vortex region as the area being contained within an ellipse in the $r - \Phi$ plane with semi-axes of $\sqrt{2 \ln(2)}\sigma_r$ and $\sqrt{2 \ln(2)}\sigma_\Phi$, thus corresponding to the full width at half maximum (FWHM) of the Gaussian fit.

This procedure was repeated for all simulation snapshots, resulting in time series data of vortex properties such as the minimum ϖ inside the vortex, the total mass enclosed in the vortex region, and the vortex location.

The algorithm is implemented in an optimized version in the *Vortector* Python package, available to the community on [github](https://github.com). The identification of vortices in a single simulation snapshot with 1058x2048 grid cells took around 50-100 ms and the fitting of the Bell curves took another 150-300 ms on modern hardware, enabling vortex detection in well over the targeted 10^6 simulation snapshots within hours of computation on a compute cluster.

Astrophysical application.

In Rometsch et al. (2021), we simulated a grid of 2D fluid dynamics models of a PPD orbiting around a solar mass star and being host to an embedded Jupiter mass planet. We varied the Shakura & Sunyaev (1973) α -viscosity parameter between 10^{-6} and 10^{-3}

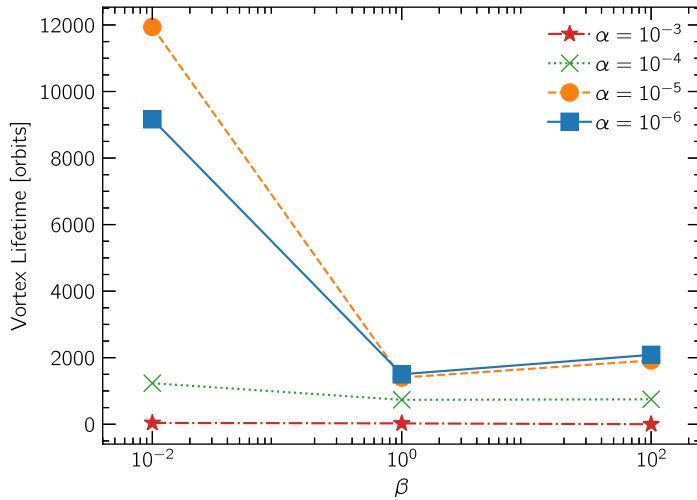


Figure 2. Dependence of vortex lifetimes on the cooling timescale β and the α viscosity parameter. The figure illustrates the existence of a long-lived regime for $\beta = 0.01$ and low viscosity $\alpha \leq 10^{-5}$. Lines are only shown to guide the eye. A simplified version of Fig. 4 in Rometsch et al. (2021) showing only the averages of the lifetimes obtained from the PLUTO and FARGO simulations.

and the β parameter between 10^{-2} and 10^2 to investigate the combined effect of the cooling timescale and viscosity on the lifetime of vortices.

The mass of the planet was increased over a period of 100 to 1000 planetary orbits to mimic giant planet formation. The growing giant planet opens a gap in the disk, and vortices appear at the edges of the gap due to the Rossby-wave instability (Lovelace et al. 1999) — in this study, we focused on the vortices located at the outer gap edge. First, multiple small vortices emerge, which usually merge into one large vortex. This large vortex then dissipates due to viscous spreading such that the lifetime increases for lower viscosities. One inquiry in the study was the lifetime of these planet-induced vortices at low values of α .

An overview of the resulting vortex lifetimes for the chosen set of parameters is shown in Fig. 2. Each model was simulated with the PLUTO (Mignone et al. 2007) and the FARGO (Masset 2000) codes, which use different numerical schemes to solve the fluid dynamics equations, to increase confidence in the validity of the numerical results.

One of the studies’ main results is the apparent existence of two regimes of vortex life at low values of viscosity. For low viscosities, $\alpha \leq 10^{-5}$, vortices in a disk with a short cooling timescale ($\beta = 0.01$) can live longer for nearly one order of magnitude compared to disks with a higher cooling timescale ($\beta \geq 1$), in agreement with earlier studies (Les & Lin 2015; Tarczay-Nehéz et al. 2020). While several possible vortex decay mechanisms other than viscous spreading exist, e.g., the elliptical instability (Lesur & Papaloizou 2009), the results hint at the existence of another vortex dispersion mechanism that depends on the thermodynamics and radiative processes of the disk and which only becomes dominant at low viscosities. The precise mechanism of vortex dissipation needs further investigation in future studies.

3. Implications

A reference for vortex characterization in simulations.

With the development of the **Vortector**, we introduced a well-defined and repeatable vortex detection and characterization algorithm. We hope that this tool provides a reproducible way for the identification and characterization of vortices in grid-based

fluid dynamics simulations of PPDs and that it facilitates the comparison of vortex properties across different studies.

Prediction for the distance at which vortices will be observed.

The cooling timescale is expected to vary in PPD, decreasing with distance from the central star from $\beta = 1 - 10$ at ~ 5 au to $\beta = 0.1 - 0.01$ at ~ 50 au (Ziampras et al. 2020). Assuming low values of viscosity and combining these expected cooling timescales with the results in Rometsch et al. (2021), planet-induced vortices can be expected to live for several ten kyrs at 5 au (in the short-lived regime for $\beta \geq 1$), several hundred kyrs at 50 au, and several Myrs at 100 au (in the long-lived regime for $\beta < 1$). Based on lifetime consideration alone, the results of our study, therefore, suggest that vortices in PPDs are more likely to be observed at large distances (≥ 50 au) from the star.

The author acknowledges funding by the Deutsche Forschungsgemeinschaft (DFG, German Research Foundation) – 325594231 and support by the High Performance and Cloud Computing Group at the Zentrum für Datenverarbeitung of the University of Tübingen, the state of Baden-Württemberg through bwHPC and the German Research Foundation (DFG) through grant INST 37/935-1 FUGG.

References

- Bae, J., Zhu, Z., & Hartmann, L. 2016, *ApJ*, 819, 134
 De Val-Borro, M., Artymowicz, P., D’Angelo, G. & Peplinski, A. 2007, *A&A*, 471, 1043
 Gammie, C. F. 2001, *ApJ*, 553, 174
 Godon, P. & Livio, M. 1999, *ApJ*, 523, 350
 Goodman, J., Narayan, R., & Goldreich, P. 1987 *MNRAS* 225, 695–711
 Les, R., & Lin, M.-K. 2015, *MNRAS*, 450, 1503
 Lesur, G., & Papaloizou, J. C. B. 2009, *A&A*, 498, 1
 Lin, M.-K., & Pierens, A. 2018, *MNRAS*, 478, 575-591
 Lovelace, R. V. E., Li, H., Colgate, S. A., & Nelson, A. F. 1999, *ApJ*, 513, 805
 Masset, F. 2000, *A&AS*, 141, 165
 Mignone, A., Bodo, G., Massaglia, S., et al. 2007, *ApJS*, 170, 228
 Miranda, R., & Rafikov, R. R. 2020, *ApJ*, 904, 121
 Pérez, L. M., Benisty, M., Andrews, S. M., et al. 2018, 2018 *ApJ*, 869, L50
 Rometsch, T., Ziampras, A., Kley, W. & Béthune, W. 2021, *A&A*, 656, A130
 Shakura, N. I., & Sunyaev, R. A. 1973, *A&A*, 500, 33
 Tarczay-Nehéz, D., Regály, Z., & Vorobyov, E. 2020, *MNRAS*, 493, 3014
 Marel, N. v. d., Dishoeck, E. F. v., Bruderer, S. et al. 2013, *Science*, 340, 1199
 Ziampras, A., Kley, W., & Dullemond, C. P. 2020, *A&A*, 637, A50

Discussion

SIMON PORTEGIES ZWART: The vortices seem to grow very quickly, very massive, then stay for a while and then sort of die out, but the quick appearance also suggests that there might be some influence by the initial conditions. How do you explain the sudden appearance of these huge vortices?

ROMETSCH: The vortex grows as the planet is introduced into the simulation, and its mass is gradually increased to mimic the gas accretion of the giant planets. The timescale is on the lower side of timescales expected for runaway accretion. We also checked for a planet growth timescale of 1000 orbits instead of 100 orbits, and the same effect appears. As soon as the giant planet opens a gap, the Rossby-wave instability kicks in, and the vortices form very quickly.

SIMON PORTEGIES ZWART: But it's a bit of a chicken and the egg problem, right? Who is first, the vortex or the planet?

ROMETSCH: Yes, it is. But you can also form vortices just by viscosity transitions alone, e.g., at a MRI dead zone. The fast vortex growth is a feature of the Rossby-wave instability rather than the planet growth process.

SHYAM MENON: You mentioned that vortices are also locations of dust traps, so you have a density peak there. Naively, one would expect that you would scale with surface density rather than its inverse when you are looking for vortices.

ROMETSCH: The background Keplerian disk has a positive vorticity contribution. The anticyclonic vortices have a negative contribution, thus they lower the vorticity. Then dividing by the surface density enhances the contrast between the background disk and vortices.